Multipartite nonlocality and symmetry breaking in one-dimensional quantum chains

Zhao-Yu Sun [*], Liang-Fu Liu, Hui-Xin Wen, Shu Qu, and Fan-Qin Xu
School of Electrical and Electronic Engineering, Wuhan Polytechnic University, Wuhan 430023, China

Bin Guo
Department of Physics, Wuhan University of Technology, Wuhan 430070, China

(Received 17 January 2023; accepted 28 April 2023; published 24 May 2023)

Multipartite nonlocality is a measure of multipartite quantum correlations. In this paper we investigate the influence of symmetry-breaking perturbations upon ground-state nonlocality by considering several typical finite-size quantum models, including the transverse-field Ising chains, the $XY(XX)$ chains, and the XXZ chains. We find that even a slight perturbation can reshape the nonlocality curve dramatically. For instance, in the XY chains, a perturbation can induce an oscillation behavior in the nonlocality curve. A clear microscopic mechanism for the results is proposed. Furthermore, we also connect the behaviors to the macroscopic symmetry properties of the chains and make some predictions on general models.

DOI: 10.1103/PhysRevA.107.052216

I. INTRODUCTION

Quantum entanglement in low-dimensional quantum systems has been investigated for more than 20 years [1,2]. In particular, bipartite quantum entanglement entropy has been widely used to characterize quantum phase transitions (QPTs) in various one-dimensional (1D) quantum chains. On the one hand, it indeed provides a valuable perspective for us to understand QPTs [3–5]. On the other hand, the corresponding findings have promoted great developments of the tensor-network algorithms and software [6–8].

For many-body quantum systems, bipartite settings may not be able to disclose all the mystery of entanglement in the systems. Thereby, multipartite quantum correlations have attracted much attention [9–18], and a recent review paper can be found in [19]. There are many approaches to characterize multipartite correlations, among which multipartite quantum nonlocality plays an important role [20–44]. Multipartite nonlocality can be detected by the violation of Bell-type inequalities. In experimental research, some remarkable progress has been made [45–49]. For instance, in Ref. [49], multipartite nonlocality in quantum systems with n up to 14 has been observed experimentally. In theoretical research, multipartite nonlocality in low-dimensional quantum chains has also attracted much attention [50–56]. Multipartite correlation measures, which aim to reveal underlying fine structures in quantum systems, are usually rather difficult to calculate. Nevertheless, multipartite nonlocality achieves a certain balance between the amount of quantum information it reveals and the amount of calculation it needs. On the one hand, nonlocality does not tend to reveal all fine structures of multipartite correlations. Instead, it uses a *hierarchy* approach [26], which may be rough but is still quite informative, to provide an overall description of multipartite correlations. Indeed, it is able to distinguish between a complete series of quantum states, i.e., from product states to genuine n-partite correlated states. On the other hand, based upon the develop of tensor-network algorithms, multipartite nonlocality can be efficiently calculated for both finite-size long quantum chains [51] and infinite-size chains [56].

Multipartite nonlocality has been used to characterize quantum correlations in various low-dimensional quantum lattices, such as 1D spin chains [50–52,57–61], Heisenberg spin ladders [54], two-dimensional quantum lattices [41,62], and many others [55]. Some general results have already been established. For instance, in typical quantum lattices, multipartite nonlocality can provide a remarkable approach to characterize both traditional QPTs [59] and some novel QPTs such as the topological QPTs [61]. Moreover, a transfer-matrix theory has been established recently, which offers a unified description about the scaling of multipartite nonlocality in translation-invariant quantum chains [56]. One can see that multipartite nonlocality provides a perspective for us to increase our knowledge about low-dimensional quantum lattices.

It deserves mention that symmetry and its breaking in quantum systems is a valuable topic [63–70]. In particular, the influence of the symmetry breaking upon quantum entanglement and quantum correlations has already been discussed in detail in several papers [67–70]. These studies mainly considered the discrete Z_2 symmetry. In our studies about multipartite nonlocality with tensor-network algorithms, the issue about symmetry breaking may have appeared vaguely, and results which seem to contradict each other were reported. That is, in finite-size transverse-field Ising chains, genuine n-partite nonlocality was observed [53], while in infinite-size transverse-field Ising chains, nonlocality was not observed in the same parameter regions [51]. These confusing results may just result from symmetry breaking. On the one hand,

[*]Corresponding author: sunzhaoyu2020@whpu.edu.cn

for finite-size chains, since good quantum numbers can be adopted easily in the numerical simulations [7,8], the converged wave functions are *symmetry-preserved ground states*. On the other hand, for tensor-network simulations of infinite-size chains, the discrete symmetry may be spontaneously broken [71], and the converged wave functions are *symmetry-broken ground states*. Thereby, our first motivation is to study whether or not the presence or absence of genuine n-partite nonlocality is related to the preservation or breaking of the symmetry in the ground states of the chains.

Our second motivation is that, in real experiments, symmetry-breaking perturbations may emerge naturally. We also take the transverse-field Ising model with $H = \sum \sigma_i^x \sigma_{i+1}^x + h \sum \sigma_i^z$, for instance, where h denotes the magnetic field and the model has a Z_2 symmetry. Nevertheless, in a real experiment, it is difficult, if possible, to apply a magnetic field to the z axis *exactly*. A slight offset of the direction of the magnetic field from the z axis (by a small angle $\theta \gtrsim 0$) would intermediately result in a perturbed Hamiltonian, such as $\tilde{H} = \sum \sigma_i^x \sigma_{i+1}^x + h \cos\theta \sum \sigma_i^z + h \sin\theta \sum \sigma_i^x$, in which the Z_2 symmetry is broken no matter how small θ is. Therefore, analysis about symmetry-breaking effects would be valuable to understand potential complex results of multipartite nonlocality in real experiments.

In this paper, we will investigate multipartite nonlocality and symmetry breaking in 1D finite-size quantum chains. To proceed, we will compare (1) chains with some symmetry and (2) chains with slight perturbations which break the symmetry. Several typical models, such as the transverse-field Ising model, the $XY(XX)$ model, and the XXZ model, will be used as our test bed. It deserves mention that not just the discrete Z_2 symmetry but also continuous symmetries will be considered. The influence of symmetry breaking upon multipartite nonlocality in these models will be characterized explicitly. Furthermore, some unexpected results, such as a symmetry-breaking-induced oscillation of multipartite nonlocality, will be reported.

This paper is organized as follows. In Sec. II the concept of multipartite nonlocality is introduced. Some numerical details are also explained. Results for the transverse-field Ising model, the $XY(XX)$ model, and the XXZ model will be reported in Sec. III, IV, and V, respectively. A summary of the paper is presented in Sec. VI.

II. BELL-TYPE INEQUALITIES AND MULTIPARTITE QUANTUM NONLOCALITY

A. A brief review of Bell inequalities

The field of Bell-type inequalities and multipartite nonlocality is still in rapid development, and there are various types of Bell inequalities in the literature [20–44]. On the one hand, for certain specific quantum states, one usually needs to construct specific Bell inequalities. For instance, the Mermin-Klyshko-Svetlichny (MKS) inequality is maximally violated by the Greenberger-Horne-Zeilinger (GHZ) state $|\psi_{\rm GHZ}\rangle = \frac{1}{\sqrt{2}}(|000\rangle + |111\rangle)$ [72]. For the W state $|\psi_{\rm W}\rangle = \frac{1}{\sqrt{3}}(|001\rangle + |010\rangle + |100\rangle)$ [73], other Bell inequalities have been constructed so as to exhibit strong violation [30]. On the other hand, the complexity of the correlation functions involved in these Bell inequalities also varies greatly. For instance, in some Bell-type inequalities, n-site full-correlations are involved [20–22]. Nevertheless, in order to facilitate experimental implementation, inequalities involving only one- and two-site expectation values have also been constructed [33,36,38–40] and have been used to characterize quantum criticality [41]. Generally speaking, a specific class of Bell inequalities just capture a subset of multipartite nonlocality that could arise in quantum systems.

In this paper, we mainly consider the MKS inequalities, which belong to the full-correlation-Bell-inequality family. As mentioned above, the MKS inequalities are violated maximally by the GHZ state and thus can be used to characterize multipartite nonlocality in GHZ-like quantum states. Moreover, previous studies [51,56] find that in various 1D translation-invariant quantum chains, the measure $\mathcal{S}$ of the MKS inequalities scales as $\mathcal{S} \sim 2^{kn}$ with $k \geqslant 0$, and thus the lowest-rank MKS inequality $\mathcal{S} \leqslant 1$ is violated strongly in most situations. Therefore, the MKS inequalities have successfully captured part of the multipartite nonlocality in typical 1D quantum chains. Advanced tensor network techniques have disclosed some insight for the success of these inequalities [74]. That is, the coefficient tensor of the MKS operator is translation-invariant, and there exists some hidden matching between the MKS operator and the ground states of translation-invariant 1D quantum chains.

It deserves mention that the violation of the MKS inequalities is a sufficient but not necessary condition for the presence of multipartite nonlocality in the concerned quantum states. Therefore, the conclusions of this paper should be restricted on the subset of multipartite nonlocality which the MKS inequalities can detect.

In the following part of this section, we will first introduce the concept of two-site Clauser-Horne-Shimony-Holt (CHSH) inequality and quantum nonlocality [31] in Sec. II B, then generalize to multipartite situations in Sec. II C. In Sec. II D we will introduce a quantity $\mathcal{K}$ which is used to characterize multipartite nonlocality in 1D translation-invariant quantum chains. Numerical details are shown in Sec. II E.

B. CHSH inequality for $n = 2$

Consider a Bell experiment where sites 1 and 2 are measured by Alice and Bob, respectively. Alice carries out one out of two possible measurements (labeled as a_1, a_1') on the site 1, and the corresponding outcome is labeled as $s_1, s_1' \in \{-1, +1\}$. On the other hand, Bob carries out one out of two possible measurements (labeled as a_2, a_2') on site 2, and the outcome is $s_2, s_2' \in \{-1, +1\}$. By repeating the experiment for many times, they obtain the expectation values of the product of the outcomes, for instance, $\langle s_1 s_2\rangle$, $\langle s_1 s_2'\rangle$, $\langle s_1' s_2\rangle$, and $\langle s_1' s_2'\rangle$. For any local realistic theory, one can prove that [31]

$$S_2(a_1, a_1', a_2, a_2') = \tfrac{1}{2}\langle s_1(s_2 + s_2')\rangle + \tfrac{1}{2}\langle s_1'(s_2 - s_2')\rangle \leqslant 1. \quad (1)$$

This inequality is called the CHSH inequality.

We shall translate Eq. (1) into the language of quantum mechanics. First, for a two-qubit quantum state described by a density matrix $\hat{\rho}_2$, we shall regard a_1 as some measurement direction $\boldsymbol{a}_1$ along which we measure the spin of site 1. If the spin turns out to be along the direction $\boldsymbol{a}_1$, we shall have $s_1 = 1$, and if the spin is along $-\boldsymbol{a}_1$, we have $s_1 = -1$. In this way, the measurement is replaced by an operator

$$\hat{s}_1 = \boldsymbol{a}_1 \cdot \boldsymbol{\sigma}, \tag{2}$$

with $\boldsymbol{\sigma} = (\hat{\sigma}^x, \hat{\sigma}^y, \hat{\sigma}^z)$. a_1', a_2, and a_2' are also treated straightforwardly.

Consequently, the CHSH inequality is translated as

$$S_2(\boldsymbol{a}_1, \boldsymbol{a}_1', \boldsymbol{a}_2, \boldsymbol{a}_2') = \mathrm{Tr}(\hat{\rho}_2 \hat{S}_2) \leqslant 1, \tag{3}$$

where the two-qubit operator $\hat{S}_2$ is defined as

$$\hat{S}_2(\boldsymbol{a}_1, \boldsymbol{a}_1', \boldsymbol{a}_2, \boldsymbol{a}_2') = \tfrac{1}{2}\hat{s}_1 \otimes (\hat{s}_2 + \hat{s}_2') + \tfrac{1}{2}\hat{s}_1' \otimes (\hat{s}_2 - \hat{s}_2'). \tag{4}$$

Furthermore, one removes any dependence on the local measures [27,57,75–77] and thus rephrases Eq. (3) as

$$\mathcal{S}_2 = \max_{\{\boldsymbol{a}_1, \boldsymbol{a}_1', \boldsymbol{a}_2, \boldsymbol{a}_2'\}} \mathrm{Tr}(\hat{\rho}_2 \hat{S}_2) \leqslant 1. \tag{5}$$

According to the local realistic theory, Eq. (5) should always hold. Nevertheless, for some quantum states $\hat{\rho}_2$, Eq. (5) can be violated. Then we can conclude that $\hat{\rho}_2$ presents some kind of quantum correlations which cannot be described by any local realistic theory, in other words, quantum nonlocality.

C. Mermin-Klyshko-Svetlichny inequalities for general *n*

1. Grouping number

In multipartite situations with $n > 2$, the structures (or patterns) of multipartite quantum nonlocality can be rather rich [26,30,32,35,75,78–81]. Let us consider multipartite nonlocality in a system consisting of merely three sites, a, b, and c. All the possible structures of nonlocality are illustrated in Fig. 1(a). First, we consider the structure $\{abc\}$. It means that the three sites can just be divided into one group, where each site shares nonlocal correlations with other sites. This structure is usually called genuine three-partite nonlocality. Second, we consider the other extreme case, the structure $\{a|b|c\}$. It means that the three sites can be divided into three groups, where no site could share any nonlocal correlation with other sites. This structure presents no nonlocality at all. Third, we consider an intermediate situation, for instance, the structure $\{a|bc\}$. It means that the three sites can be divided into two groups, where the site a is in one group and the sites b and c are in the other group. Only b and c share nonlocal correlations with each other. Thus, for all other structures in Fig. 1, their physical meaning can be understood straightforwardly.

These structures indeed provide a fine description of multipartite nonlocality for small n. Nevertheless, when n is very large, the structures would become so rich that analyzing the structures becomes intractable. An alternative approach is to use the grouping number g [26]. It is clear that the grouping number of $\{abc\}$ is $g = 1$, the grouping numbers of $\{a|bc\}$, $\{ab|c\}$, and $\{ac|b\}$ are $g = 2$, and the grouping number of $\{a|b|c\}$ is $g = 3$. Using this approach, for general n, all the structures can always be classified into n families labeled by $g = 1, 2, \ldots, n$. The physical meaning of g is also quite clear, that is, a larger (smaller) value of g (with $1 \leqslant g \leqslant n$) denotes a lower (higher) hierarchy of multipartite nonlocality.

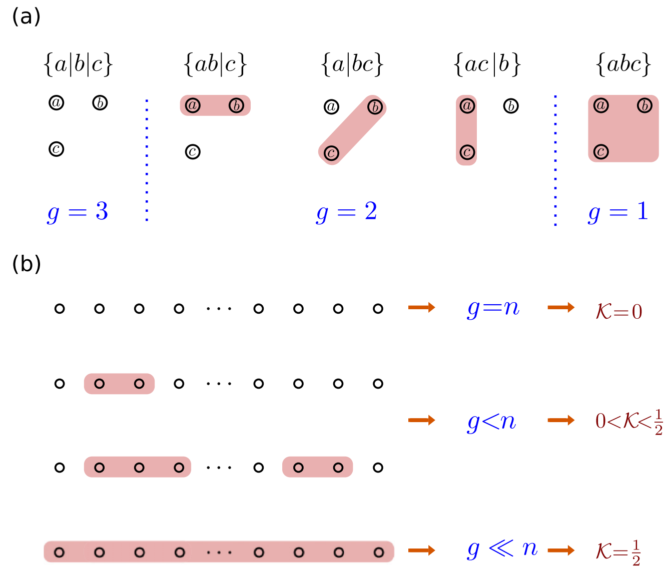

FIG. 1. (a) Various patterns of multipartite nonlocality in three-site systems consisting of sites a, b, and c. Pink shadings indicate the groups in which the sites can share nonlocal correlations with each other. The grouping number g offers a rough approach to classifying these structures. (b) In 1D quantum chains, a quantity $\mathcal{K} \in [0, \frac{1}{2}]$ is more convenient to characterize multipartite nonlocality. $\mathcal{K} = 0$ indicates that no nonlocality is observed by current Bell inequality, and $\mathcal{K} = \frac{1}{2}$ indicates high-hierarchy multipartite nonlocality.

2. Mermin-Klyshko-Svetlichny inequalities

For general n-qubit quantum state $\hat{\rho}_n$, its grouping number g can be detected by MKS inequalities. To proceed similarly to Eq. (2) for each qubit i with $i = 1, 2, \ldots, n$, one defines two local operators as

$$\hat{s}_i = \boldsymbol{a}_i \cdot \boldsymbol{\sigma},$$
$$\hat{s}_i' = \boldsymbol{a}_i' \cdot \boldsymbol{\sigma}. \tag{6}$$

Then the n-qubit MKS operator $\hat{S}_n$ can be recursively defined as [20–22,26,78]

$$\hat{S}_n(\boldsymbol{a}_1, \boldsymbol{a}_1', \ldots, \boldsymbol{a}_n, \boldsymbol{a}_n') = \tfrac{1}{2}\hat{S}_{n-1} \otimes (\hat{s}_n + \hat{s}_n') + \tfrac{1}{2}\hat{S}_{n-1}' \otimes (\hat{s}_n - \hat{s}_n'). \tag{7}$$

One may see that $\hat{S}_n$ is an n-qubit generalization of the two-qubit operator $\hat{S}_2$ in Eq. (4).

For a general $\hat{\rho}_n$, suppose its grouping number is g, then the following MKS inequalities should always hold [26]:

$$\mathcal{S}_n = \begin{cases} \max_{\{\underline{a}\}} \mathrm{Tr}(\hat{\rho}_n \hat{S}_n) \leqslant 2^{\frac{n-g}{2}}, & \text{for n- g even}, \\ \max_{\{\underline{a}\}} \mathrm{Tr}(\hat{\rho}_n \hat{S}_n^+) \leqslant 2^{\frac{n-g}{2}}, & \text{for n- g odd}, \end{cases} \tag{8}$$

where $\{\underline{a}\}$ denotes the set of $2n$ unit vectors $\{\boldsymbol{a}_1, \boldsymbol{a}_1', \ldots, \boldsymbol{a}_n, \boldsymbol{a}_n'\}$ and $\hat{S}_n^+ = (\hat{S}_n + \hat{S}_n')/\sqrt{2}$. It is clear that the CHSH inequality in Eq. (5) can be regarded as an instance of the MKS inequalities with $n = g = 2$.

If Eq. (8) is violated, the grouping number of the state $\hat{\rho}_n$ would be (at most) $g - 1$. Therefore, these MKS inequalities with $g = 2, 3, \ldots, n$ form a complete series. The lowest rank one is just

$$\mathcal{S}_n \leqslant 1. \tag{9}$$

If it is not violated, no quantum nonlocality is observed by the current Bell-type inequality. If it is violated, $\hat{\rho}_n$ presents (at least) the lowest hierarchy of multipartite nonlocality.

The highest rank one is

$$\mathcal{S}_n \leqslant 2^{\frac{n-2}{2}}. \tag{10}$$

If it is violated, the grouping number would just be 1. In other words, $\hat{\rho}_n$ presents the highest hierarchy of multipartite nonlocality, genuine n-partite nonlocality.

For a given quantum state, one figures out the measure $\mathcal{S}_n$, and then the grouping number g can be indicated by

$$g = n - \lceil 2\log_2 \mathcal{S}_n \rceil. \tag{11}$$

As we have mentioned, the violation of the Bell-type inequality in Eq. (8) is only a sufficient but not necessary condition for the presence of multipartite nonlocality. Consequently, Eq. (11) provides just an upper bound for the grouping number.

D. Multipartite nonlocality quantity $\mathcal{K}$ in 1D quantum chains

In this paper we consider global multipartite nonlocality of the ground states $|\psi_g\rangle$ of a special class of quantum systems, 1D quantum chains with a large n. In most situations, we are not interested in the specific value of the grouping number. Instead, a qualitative analysis of multipartite nonlocality would be sufficient to capture the ground-state properties of the chains. Thereby, we ignore the parity of $n-g$ in Eq. (8) and consider just the case where $n-g$ is an even number.

In quantum lattice theory, we are usually interested in the large-n behavior. Nevertheless, both the grouping number g and the measure $\mathcal{S}_n$ may diverge in the large-n limit. Therefore, it may be valuable to construct some quantity which needs to (1) keep finite in the large-n limit and (2) be informative. At first glance, it is intuitive to consider the quantity

$$\mathcal{G} = \lim_{n\to\infty} \frac{g}{n}. \tag{12}$$

Generally, one has

$$0 \leqslant \mathcal{G} \leqslant 1. \tag{13}$$

$\mathcal{G}$ is quite informative, that is, a *larger* value of $\mathcal{G}$ denotes a lower hierarchy of multipartite nonlocality.

With Eq. (11), one can easily figure out $\mathcal{G}$ by the calculation quantity $\mathcal{S}_n$ as

$$\begin{aligned}\mathcal{G} &= \lim_{n\to\infty} \frac{n - \lceil 2\log_2 \mathcal{S}_n \rceil}{n} \\ &= 1 - \lim_{n\to\infty} \frac{\lceil 2\log_2 \mathcal{S}_n \rceil}{n} \\ &= 1 - 2\lim_{n\to\infty} \frac{\log_2 \mathcal{S}_n}{n}. \end{aligned} \tag{14}$$

It becomes convenient to define $\frac{\log_2 \mathcal{S}_n}{n}$ as a new quantity,

$$\mathcal{K} = \frac{\log_2 \mathcal{S}_n}{n}, \tag{15}$$

and then one will have

$$\mathcal{G} = 1 - 2\lim_{n\to\infty} \mathcal{K}. \tag{16}$$

According to Eqs. (13) and (16), it is clear that

$$0 \leqslant \lim_{n\to\infty} \mathcal{K} \leqslant \tfrac{1}{2}. \tag{17}$$

Compared with $\mathcal{G}$, $\mathcal{K}$ seems to be a more intuitive quantity for characterizing multipartite nonlocality, that is, a *larger* value of $\mathcal{K}$ denotes a *higher* hierarchy of multipartite nonlocality.

It is worth noting that $\mathcal{K}$ has a close connection with the scaling behavior of $\mathcal{S}_n$. In various 1D translation-invariant quantum chains, $\mathcal{S}_n$ scales as [51,56]

$$\log_2 \mathcal{S}_n \sim kn + b, \tag{18}$$

where the slope k and the intercept b are n-independent. Comparing Eqs. (15) and (18), one can see that $\lim_{n\to\infty} \mathcal{K}$ is just the slope k in this scaling formula.

Based upon the above considerations, we will use the quantity $\mathcal{K}$ to characterize multipartite nonlocality in 1D quantum chains in this paper.

E. Numerical details

The concerned state is the ground states $|\psi_g\rangle$ of the quantum chains. Thus, in Eq. (8), $\hat{\rho}_n$ shall be rephrased as $\hat{\rho}_n = |\psi_g\rangle\langle\psi_g|$, and the expectation value $\mathrm{Tr}(\hat{\rho}_n\hat{S}_n)$ shall be rephrased as $\langle\psi_g|\hat{S}_n|\psi_g\rangle$. Moreover, the number n is just the length N of the chains.

Our numerical calculations consist of two steps. In the first step, we need to figure out the ground states $|\psi_g\rangle$. When $N \leqslant 12$, we figure out $|\psi_g\rangle$ exactly by exact diagonalization. When $N > 12$, we use Itensor [8] to figure out the ground-state wave functions $|\psi_g\rangle$ of the concerned 1D quantum chains in the form of matrix product states (MPSs) [7]. When no additional specifications are given, we consider N-site chains with an even N and with open boundary conditions. When optimizing the MPSs, we set the maximal bond dimension as $\chi = 200$, and we always sweep the lattices up to 100 times so as to ensure the convergence of the wave functions. Moreover, when Z_2 symmetry is present in the chains, we use the symmetry in our calculation as as to improve the accuracy of the wave functions [8].

In the second step, we figure out the global multipartite nonlocality measure $\mathcal{S}_n$ for the ground states $|\psi_g\rangle$. According to Eq. (8), one needs to carry out a global optimization of $f(\boldsymbol{a}_1, \boldsymbol{a}'_1, \ldots, \boldsymbol{a}_n, \boldsymbol{a}'_n) = \langle\psi_g|\hat{S}_n(\boldsymbol{a}_1, \boldsymbol{a}'_1, \ldots, \boldsymbol{a}_n, \boldsymbol{a}'_n)|\psi_g\rangle$ with respect to $2n$ unit vectors. This problem has been solved by the two-site update algorithm proposed in [51]. The basic idea is that, in each step of the optimization, one just optimizes the objective function f with respect to the four vectors $\boldsymbol{a}_i, \boldsymbol{a}'_i, \boldsymbol{a}_{i+1}$, and $\boldsymbol{a}'_{i+1}$ on two sites i and $i+1$, with all the other $2n-4$ vectors fixed. After a solution is figured out, one updates the vectors on these two sites and moves on to optimize vectors on the next two sites. One sweeps the entire lattice for several times until some convergence is obtained. In practice, the two-site update algorithm may be trapped in some local minimum. The issue can be overcome by adopting multirandom initial points and carrying out the optimizations independently for many rounds. In our calculation in this

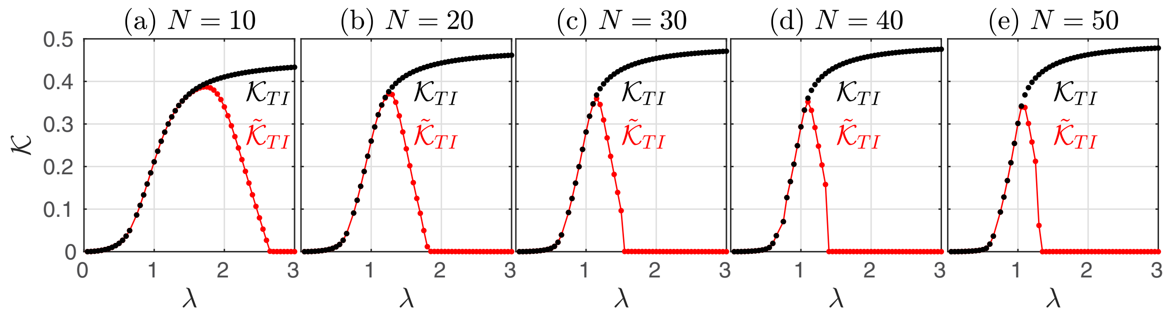

FIG. 2. Multipartite nonlocality in finite-size transverse-field Ising chains (i.e., $H = \lambda \sum \sigma_i^x \sigma_{i+1}^x + \sum \sigma_i^z$), with N the length of the chains and λ the reciprocal of the magnetic field. $\lambda_c = 1$ is the critical point in the thermodynamic limit. $\mathcal{K}_{TI}(\lambda)$ corresponds to the original Z_2-symmetric chain, and it increases monotonously. $\tilde{\mathcal{K}}_{TI}$ corresponds to the chain whose Z_2 symmetry is broken by a slight perturbation (i.e., $H_x' = \delta \sum \sigma_i^x$ with $\delta = 10^{-4}$). Nonlocality is destroyed dramatically by the perturbation for $\lambda > 1$, and consequently $\tilde{\mathcal{K}}_{TI}(\lambda)$ presents a sharp peak in the vicinity of $\lambda_c = 1$ in the large-N limit.

paper, for each set of physical parameters, we always carry out 20 rounds of optimizations independently. Finally, we use Eq. (15) to figure out $\mathcal{K}$.

In this paper both chains with some symmetry-breaking perturbations and chains without perturbation will be considered. Thus, it may be helpful to state some conventions in advance. Chains without perturbation will be called the *original* chains. The corresponding model Hamiltonian and the nonlocality measure will be denoted by H and $\mathcal{K}$, respectively. When some perturbations are taken into account, the chains will be called the *perturbed* chains. Then the Hamiltonian and the nonlocality measure will be denoted by $\tilde{H}$ and $\tilde{\mathcal{K}}$, respectively.

III. TRANSVERSE-FIELD ISING MODEL

The first toy model is the 1D transverse-field Ising model. Although it seems to be an overly simple model, it is valuable to clarify some confusing results reported previously in finite and infinite-size chains [51,53]. More importantly, the corresponding mechanism will offer a cornerstone for us to analyze more complex results in the next sections.

The Hamiltonian of the model is given by

$$H = J \sum_{i=1}^{N-1} \sigma_i^x \sigma_{i+1}^x + h \sum_{i=1}^{N} \sigma_i^z, \tag{19}$$

where J is the spin-spin coupling constant and h is the strength of the magnetic field. The phenomenon which attracts our attention occurs in the low-field regions. Therefore, in order to offer a better description of our results, we parametrize the Hamiltonian as

$$H_{TI} = \lambda \sum_{i=1}^{N-1} \sigma_i^x \sigma_{i+1}^x + \sum_{i=1}^{N} \sigma_i^z, \tag{20}$$

with $\lambda = \frac{J}{h}$ the reciprocal of the magnetic field. It is clear that when λ decreases from ∞ to 0, the system undergoes a magnetization (or polarization) process. In the thermodynamic limit, a QPT occurs at the critical point $\lambda_c = 1$. The system has a Z_2 symmetry, that is, the Hamiltonian remains unchanged when the model is rotated around the z axis by π. This Z_2 symmetry is spontaneously broken in the phase $\lambda > \lambda_c$ when $N \to \infty$.

For the original finite-size Ising chains, the multipartite nonlocality has been analyzed in detail in Ref. [53]. We still present the results in this paper, so as to compare them with the perturbed chains.

The nonlocality curve $\mathcal{K}_{TI}(\lambda)$ is illustrated in Fig. 2, with N up to 50. One sees that $\mathcal{K}_{TI}$ increases monotonously from 0 (with $\lambda = 0$) to $\frac{1}{2}$ (with $\lambda \to \infty$). It captures the process in which the ground states gradually change from product states to highly nonlocal states. [Detailed analysis shows that the highest-rank MKS inequality in Eq. (10) is indeed violated, thus genuine n-partite nonlocality is observed.] Moreover, when N is large enough, the $\mathcal{K}_{TI}(\lambda)$ curves with different N tend to overlap with each other. It means that the behavior in the thermodynamic limit is captured. Thereby, we have established an overall description about nonlocality in the original Ising chains with the quantity $\mathcal{K}_{TI}$.

When a symmetry-breaking perturbation is present, the behavior could change dramatically. We consider a perturbed model given by

$$\tilde{H}_{TI} = H_{TI} + H_x', \tag{21}$$

where the slight perturbation is described by

$$H_x' = \delta \sum_i \sigma_i^x, \tag{22}$$

with a perturbation strength $\delta = 10^{-4}$. The effect of changing the value of δ will be discussed in next section. It is clear that this perturbation breaks the Z_2 symmetry of the chains. The corresponding numerical results $\tilde{\mathcal{K}}_{TI}(\lambda)$ are also shown in Fig. 2, where the $\tilde{\mathcal{K}}_{TI}(\lambda)$ curves are not monotonous anymore. Instead, they present a peak. When N is large enough, the peak locates in the vicinity of $\lambda_c = 1$.

By comparing $\mathcal{K}_{TI}(\lambda)$ and $\tilde{\mathcal{K}}_{TI}(\lambda)$, we can see that when N is large enough, in the phase $\lambda < \lambda_c$ the nonlocality is nearly unaffected by the perturbation, and for $\lambda > \lambda_c$ the nonlocality is dramatically destroyed by the perturbation. The underlying mechanics can be clarified by considering two extremes, i.e., $\lambda = 0$ and $\lambda \to \infty$. When $\lambda = 0$, the ground state of the original chain is $|\downarrow\downarrow \cdots \downarrow\downarrow\rangle$, where $|\downarrow\rangle$ is an eigenstate of the Pauli operator σ^z with eigenvalue -1. Considering the Z_2 symmetry, if one rotates this state around the z axis by π, one would get a state with the same energy. Nevertheless, it is clear that the rotation just produces the same state. In other words, this ground state is *unique*. Therefore, the results conform to the first-order perturbation theory, $|\mathcal{K}_{TI}(\lambda) - \tilde{\mathcal{K}}_{TI}(\lambda)| \sim \delta$. That is why the ground-state nonlocality is quite robust against perturbations when δ is rather small. When $\lambda \to \infty$, the situation is quite different. It is clear that a ground state is, for instance, $|1010\cdots1010\rangle$, where $|1\rangle$ and $|0\rangle$ are the eigenstates of the Pauli operator σ^x. Considering the Z_2 symmetry, when one rotates this state around the z-axis by π, one would get another state $|0101\cdots0101\rangle$ with the same energy. In other words, the ground states are *degenerate*. Thereby, the first-order perturbation theory is not applicable any more. Instead, the ground states may be influenced dramatically or slightly by the perturbations, depending upon the nature of the perturbations. For the perturbation H_x' considered in this paper, it breaks the Z_2 symmetry and lifts the degeneracy. That is why the ground-state nonlocality is influenced dramatically by the perturbation.

Based upon the above results, we conclude that Z_2-symmetry-breaking perturbation indeed greatly affects the presence or absence of genuine n-partite nonlocality in finite-size chains.

Z_2 symmetry is just a discrete symmetry. We mention that in quantum lattices, continuous symmetries can also emerge naturally. Therefore, in next sections, we will consider continuous symmetries. We will show that continuous symmetries play a quite interesting role in the behavior of multipartite nonlocality in perturbed 1D quantum chains.

IV. *XY* MODEL

We consider the 1D XY model described by the Hamiltonian

$$H_{XY} = \lambda \sum_{i=1}^{N-1}\left(\frac{1+\gamma}{2}\sigma_i^x\sigma_{i+1}^x + \frac{1-\gamma}{2}\sigma_i^y\sigma_{i+1}^y\right) + \sum_{i=1}^{N}\sigma_i^z, \tag{23}$$

where λ is the reciprocal of the magnetic field, and γ is the anisotropic parameter in the x-y plane. When $\gamma = 1$, the model reduces into the transverse-field Ising model studied in the previous section. When $\gamma = 0$, the model transforms into the XX model,

$$H_{XX} = \frac{\lambda}{2}\sum_{i=1}^{N-1}\left(\sigma_i^x\sigma_{i+1}^x + \sigma_i^y\sigma_{i+1}^y\right) + \sum_{i=1}^{N}\sigma_i^z, \tag{24}$$

which has a U(1) symmetry, i.e., rotation invariance in the x-y plane. On the other hand, for general $0 < \gamma < 1$, the model would have a Z_2 symmetry, just as in the transverse-field Ising model.

From the point of view of symmetry, H_{XX} (with $\gamma = 0$) and H_{XY} (with $0 < \gamma < 1$) belong to two different classes, and therefore the two are often considered separately [69]. Nevertheless, as we will show, when a perturbation exists, the nonlocality curve of finite-size XY chains can exhibit an interesting oscillation, which is closely related to the breaking of the U(1) symmetry of the XX model.

In the following parts, we will first report some accurate results for the original XY chains by considering just $N = 12$, and then take perturbations into account. After that, the mechanisms behind the numerical results will be analyzed.

A. Original *XY* chains

First of all, we consider the original model defined in Eq. (23) without any perturbation. The numerical results $\mathcal{K}(\lambda)$ with $N = 12$ are illustrated in Fig. 3. We use $\mathcal{K}_{XX}$, $\mathcal{K}_{XY}$, and $\mathcal{K}_{TI}$ to denote the results with $\gamma = 0$, $0 < \gamma < 1$, and $\gamma = 1$, respectively. In Fig. 3(a), $\mathcal{K}_{XX}(\lambda)$ exhibits a series of plateaus. This behavior results from the U(1) symmetry of the model. Because of this continuous symmetry, the Hilbert space is divided into many subspaces, and the ground state resides in some of these subspaces, depending upon the magnetic field (i.e., λ). As λ changes, the ground state jumps between these subspaces, and then the nonlocality quantity $\mathcal{K}_{XX}(\lambda)$ also changes suddenly. It needs to be mentioned that the magnetic-field term (i.e., $\sum_{i=1}^{N}\sigma_i^z$) commutes with the Hamiltonian, and thus the magnetic field just modifies the eigenvalues of the Hamiltonian but does not change the eigenstates. Thereby, in each subspace, the ground state (and consequently the ground-state nonlocality) keeps constant. That is why $\mathcal{K}_{XX}(\lambda)$ exhibits a series of plateaus in Fig. 3(a).

For $\gamma = 0.2$ in Fig. 3(b), where the U(1) symmetry is absent, we observe two results. First, $\mathcal{K}_{XY}(\lambda)$ does not exhibit any plateau anymore. It reveals that the magnetic-field term does not commute with the Hamiltonian and thus the magnetic field affects the eigenstates of the model. Second, compared with $\mathcal{K}_{XX}(\lambda)$, the sudden changes in $\mathcal{K}_{XY}(\lambda)$ become weakened. In fact, in Fig. 3, when γ increases further, the $\mathcal{K}_{XY}(\lambda)$ curve becomes smooth gradually.

B. Perturbed chains with $\delta = 10^{-4}$

Next, we consider a perturbed XY model described by

$$\tilde{H}_{XY} = H_{XY} + H_x', \tag{25}$$

where the perturbation is also given by

$$H_x' = \delta\sum\sigma_i^x, \tag{26}$$

with $\delta = 10^{-4}$. The corresponding results $\tilde{\mathcal{K}}(\lambda)$ are illustrated in Fig. 3.

For $\gamma = 0$ in Fig. 3(a), where the original model has U(1) symmetry, the nonlocality is nearly unaffected by the perturbation, i.e., $\tilde{\mathcal{K}}_{XX}(\lambda) \approx \mathcal{K}_{XX}(\lambda)$.

For $\gamma = 0.2$ in Fig. 3(b), in the vicinity of the level-crossing points [indicated by the sudden changes of $\mathcal{K}_{XY}(\lambda)$], the nonlocality suffers dramatic influence from the perturbation, and $\tilde{\mathcal{K}}_{XY}(\lambda)$ presents rather sharp valleys.

For $\gamma = 0.4$ in Fig. 3(c), $\tilde{\mathcal{K}}_{XY}(\lambda)$ is further modified and presents an oscillation behavior, i.e., multibroad peaks and sharp valleys.

When γ increases from $\gamma = 0.6$ in Fig. 3(d) to $\gamma = 1$ in Fig. 3(h), one can see that (1) most of the peaks in $\tilde{\mathcal{K}}_{XY}(\lambda)$ are weakened gradually and disappear but (2) the leftmost peak gradually rises and finally transforms into the single peak in $\tilde{\mathcal{K}}_{TI}(\lambda)$ reported in the previous section.

C. Perturbed chains with various δ

The phenomenon with $\delta = 10^{-4}$ in Fig. 3 is quite rich; for instance, the oscillation is observed for some γ but is absent for other γ. At first glance, the underlying mechanism is not clear. Testing other strengths of the perturbation may help us

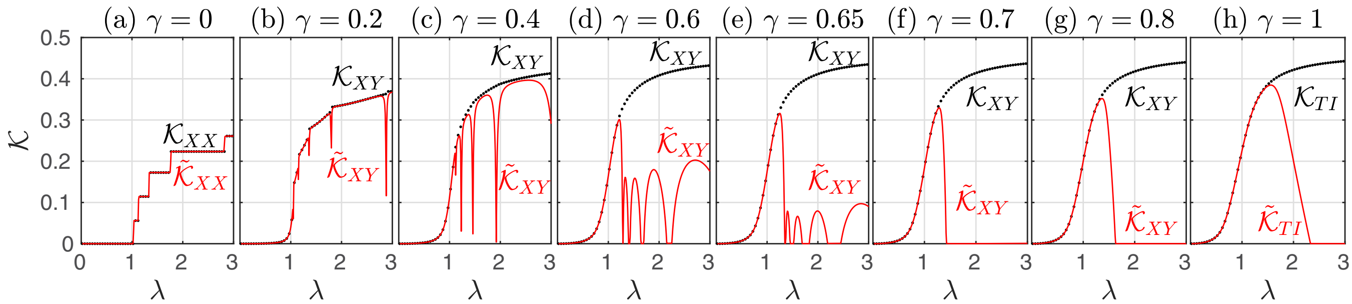

FIG. 3. Multipartite nonlocality in finite-size XY chains, $H = \lambda \sum[(1+\gamma)\sigma_i^x\sigma_{i+1}^x + (1-\gamma)\sigma_i^y\sigma_{i+1}^y] + \sum \sigma_i^z$, with $N = 12$. γ is the anisotropic parameter and λ is the reciprocal of the magnetic field. $\lambda_c = 1$ is the critical point for infinite-size chains. $\mathcal{K}_{XX}$, $\mathcal{K}_{XY}$, and $\mathcal{K}_{TI}$ correspond to the original chains with various γ. For $\gamma = 0$, the chain has a U(1) symmetry, and thus $\mathcal{K}_{XX}(\lambda)$ exhibits step-by-step changes. For $\gamma > 0$, the U(1) symmetry is broken, and $\mathcal{K}_{XY}(\lambda)$ becomes smooth gradually. $\tilde{\mathcal{K}}_{XX}$, $\tilde{\mathcal{K}}_{XY}$, and $\tilde{\mathcal{K}}_{TI}$ correspond to the chains with a Z_2-breaking perturbation $H_x' = \delta \sum \sigma_i^x$ with $\delta = 10^{-4}$. With $\gamma = 0$, $\tilde{\mathcal{K}}_{XX}(\lambda)$ is almost unaffected by the perturbation. With $\gamma = 0.2$, $\tilde{\mathcal{K}}_{XY}(\lambda)$ suffers dramatic influence from the perturbation at some λ/s and presents rather sharp valleys. As γ increases further (i.e., $\gamma < 0.7$), $\tilde{\mathcal{K}}_{XY}(\lambda)$ exhibits an oscillation behavior. This oscillation is related to the breaking of both U(1) and Z_2 symmetries.

to find some clues. Therefore, in Fig. 4 we take the chain with $\gamma = 0.65$ as an example, and illustrate the nonlocality curves for various δ. Results for the original XY chain (i.e., $\delta = 0$) are also shown for comparison. It is clear that the value of δ has a strong modulation effect upon the oscillation behavior. When δ is rather large ($\delta = 10^{-4}$), the nonlocality is destroyed in some regions. When δ is small enough ($\delta = 10^{-6}$), nevertheless, a complete oscillation curve is recovered. These results reveal that the presence or absence of the oscillation in Fig. 3 is not an *inherent* characteristic of the corresponding models. Instead, it may depend upon the relative strength between the external perturbations and some internal property, such as the energy gap, of the chains.

D. Microscopic mechanisms: Interplay between perturbation and energy gap

In order to clarify the *microscopic* mechanisms for these oscillations in detail, we have additionally illustrated the corresponding energy gap ΔE for both the original chains and the perturbed chains in Fig. 5. By comparing the nonlocality curves (Fig. 3) and the energy gap curves (Fig. 5), we find that there are two mechanisms for how the oscillation occurs in the model. First, the model has a series of energy-level crossings. In fact, it is clear that there is a one-to-one correspondence between the sharp valleys of $\tilde{\mathcal{K}}_{XY}(\lambda)$ in Figs. 3(b) and 3(c) and the level crossings (where the energy gap vanishes) in Figs. 5(b) and 5(c). Second, the energy gap needs to be rather small. For $\gamma = 0$ in Fig. 5(a), the energy gap is quite large. Consequently, a slight perturbation is not sufficient to destroy the ground state, and thus we have $\tilde{\mathcal{K}}_{XX}(\lambda) \approx \mathcal{K}_{XX}(\lambda)$ in Fig. 3(a). When γ increases, nevertheless, as shown in Fig. 5, the $\Delta E(\lambda)$ curve is suppressed ambiguously, especially in the vicinity of the level-crossing points. Then, if some perturbation is imposed, the ground state can be influenced considerably. Consequently, in the vicinity of *each* level-crossing point, we find $\tilde{\mathcal{K}}_{XY}(\lambda) \ll \mathcal{K}_{XY}(\lambda)$. That is why $\tilde{\mathcal{K}}_{XY}(\lambda)$ presents multiple sharp valleys for $\gamma = 0.4$ in Fig. 3(c).

It is reasonable that the influence of the perturbation upon the ground state depends upon the relative strength of the perturbation with respect to the energy gap,

$$\frac{\delta}{\Delta E}. \tag{27}$$

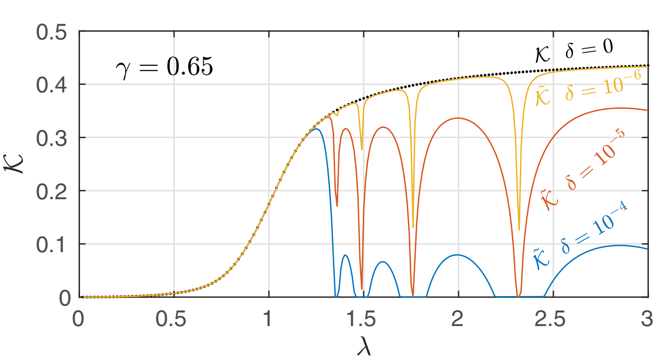

FIG. 4. Multipartite nonlocality in XY chains (with $N = 12$ and $\gamma = 0.65$) for various perturbation strength δ.

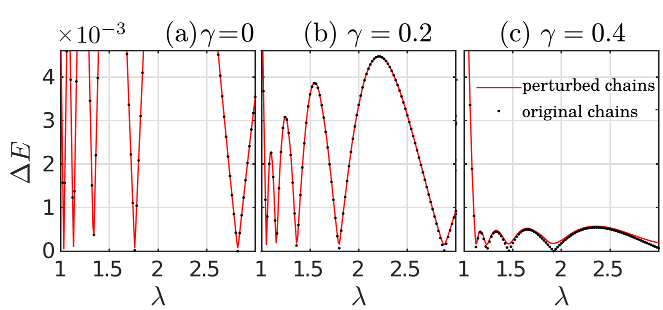

FIG. 5. Energy gap ΔE in finite-size XY chains with $N = 12$. The black dots correspond to the original XY model without perturbation. At some special λ/s, the gap is closed, which indicates ground-state level crossings. As γ increases from (a) to (c), the $\Delta E(\lambda)$ curve is suppressed ambiguously. Red solid lines correspond to the perturbed chains with $H_x' = \delta \sum \sigma_i^x$ with $\delta = 10^{-4}$. When γ is large enough (which means ΔE is small enough), the perturbation has considerable influence upon the energy gap in the vicinity of the level-crossing points, for instance, $\lambda = 1.92$ in (c).

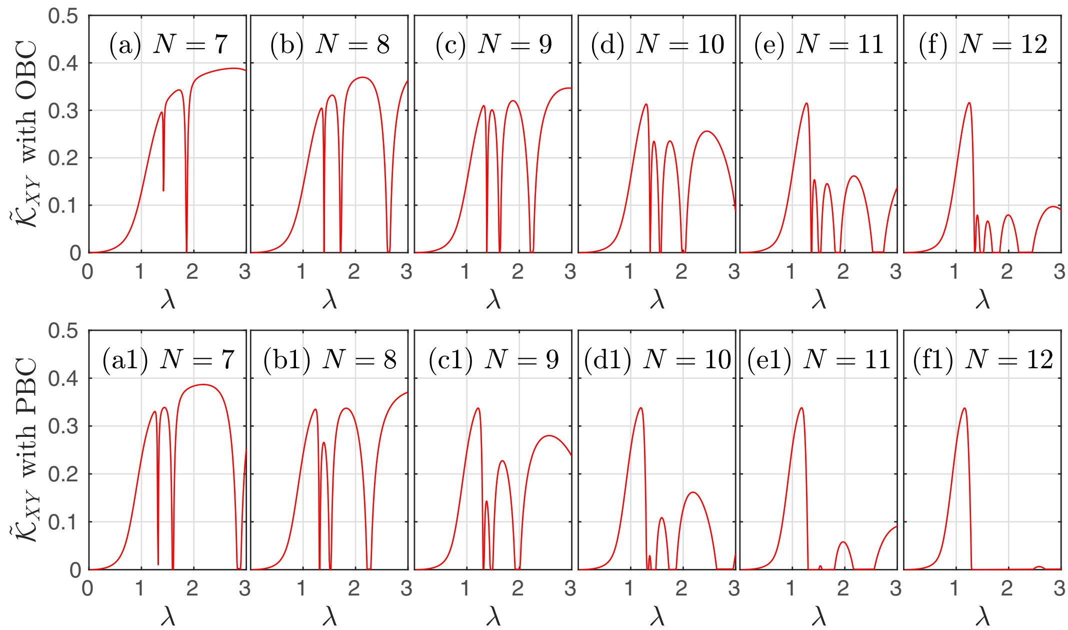

FIG. 6. Finite-size effects of multipartite nonlocality in XY chains with a Z_2-breaking perturbation $H_x' = \delta \sum \sigma_i^x$ for various N. The anisotropic parameter is $\gamma = 0.65$, and the perturbation strength is $\delta = 10^{-4}$. Both open boundary conditions [(a)–(f)] and periodic boundary conditions [(a1)–(f1)] are considered. As N increases, the oscillations become more frequent, and the $\tilde{\mathcal{K}}_{XY}(\lambda)$ curve is suppressed. The underlying mechanism is explained in the text.

When $\frac{\delta}{\Delta E} \to 0$, the perturbation effect would be little, and when $\frac{\delta}{\Delta E} \to \infty$, the perturbation effect would be significant. We mention that in the XY chains, as γ increases, the energy gap ΔE becomes smaller. In other words, for fixed $\delta = 10^{-4}$, $\frac{\delta}{\Delta E}$ is enhanced gradually. That is why as γ increases the $\tilde{\mathcal{K}}_{XY}(\lambda)$ curve is suppressed gradually and the oscillation vanishes finally in Fig. 3. In this way, all the phenomena in Fig. 3 have a clear and consistent explanation.

E. Finite-size effects

We would like to mention that the microscopic mechanisms revealed above can help us to carry out some valuable qualitative analysis. For instance, one may wonder what would happen in chains with a large N. For the XY model with $\gamma \neq 1$, when we give our attention to the energy spectrum, it is easy to check that as N increases, there are two key finite-size effects:

(i) The number of level crossings would be increased.

(ii) The energy gap ΔE would be decreased.

In fact, for a small N, there will be an ambiguous step-by-step change in the behavior of any observable (such as the magnetic moment and multipartite nonlocality). For a large N, nevertheless, the number of level crossings would be rather large, and the step-by-step change in the observable curve would become smooth gradually.

These two finite-size effects about the energy spectrum can help us to figure out the finite-size effects on multipartite nonlocality. First, since the oscillation is related to the energy-level crossings, the finite-size effect (i) immediately causes the oscillations to become even more frequent when N is large. Second, since the influence of the perturbation upon nonlocality is determined by the relative strength $\frac{\delta}{\Delta E}$, the finite-size effect (ii) indicates that when N increases, the destructive influence of the perturbation upon ground-state nonlocality would become stronger, in other words, the nonlocality quantity would become smaller. These two behaviors have been confirmed ambiguously in Fig. 6 by considering models with $N = 7, 8, 9, \ldots, 12$, and with both open boundary conditions (OBCs) and periodic boundary conditions (PBCs).

Moreover, in Fig. 7 we have shown numerical results with N up to 50. Let us first consider, for instance, $\gamma = 0.2$. We have already shown that $\tilde{\mathcal{K}}_{XY}$ is quite close to $\mathcal{K}_{XY}$ when $N = 12$ in Fig. 3(b). With $N = 50$ in Fig. 7(b), the difference between $\tilde{\mathcal{K}}_{XY}$ and $\mathcal{K}_{XY}$ becomes much larger. In other words, as N increases, the perturbation effect is indeed enhanced, which is consistent with our above qualitative analysis. Then we turn our attention to $\gamma = 0.4$. One can see that compared with $N = 12$ in Fig. 3(c), the effect of the perturbation with $N = 50$ in Fig. 7(c) is so strong that the oscillation is completely destroyed. We would like to mention that according to our theory, the oscillation can always be recovered as long as the relative strength $\frac{\delta}{\Delta E}$ is appropriate, for instance, by decreasing the perturbation strength δ.

F. Role of symmetries

While the *microscopic* energy-level structures have indeed offered us a unified explanation, it would also be valuable to connect the oscillation behavior to some *macroscopic* properties of the chains, so as to help us to generalize the observations to some other models which present similar macroscopic properties. We argue that the emergence of the oscillations is associated with the breaking of the symmetries in the chains. First, for the finite-size XX chains with U(1) symmetry, the energy gap is large. In this situation,

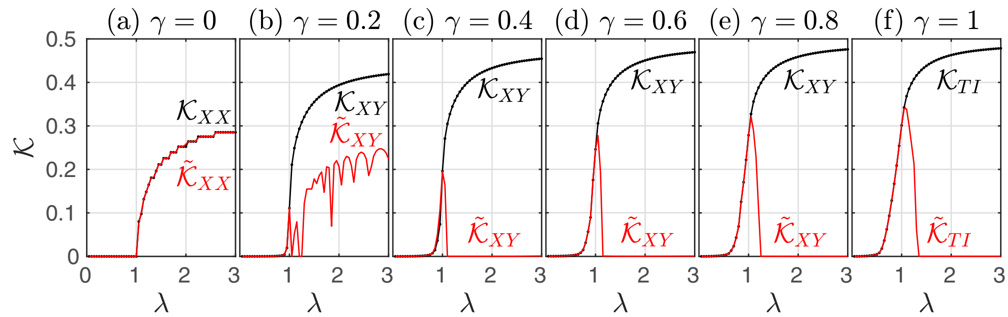

FIG. 7. Multipartite nonlocality in finite-size XY chains. All the settings are consistent with Fig. 3, except $N = 50$. It suggests that when N is large, the oscillation in $\tilde{\mathcal{K}}_{XY}(\lambda)$ tends to be observed in chains with a small nonzero γ [which slightly breaks the U(1) symmetry] and an additional perturbation H'_x (which breaks the Z_2 symmetry).

the ground state (and the ground-state nonlocality) is robust against slight perturbations. However, just because of this U(1) symmetry, as we have explained, under the magnetic field, the ground-state energy would undertake a series of level crossings. Second, when this U(1) symmetry is slightly broken and is reduced into a Z_2 symmetry, these level crossings are kept, but the corresponding energy gap is weakened gradually. This makes it possible for the ground state to be destroyed by slight perturbations. Third, in the vicinity of *each* level-crossing point of the Z_2-symmetric chains, when a Z_2-breaking perturbation is imposed, the ground state can be easily destroyed, and then the nonlocality curve would present a sharp valley.

According to the above discussions, we expect that the oscillation of nonlocality may also be observed in some other finite-size models. One can (i) find a U(1)-symmetric lattice under a magnetic field, (ii) use anisotropy to break the U(1) symmetry so as to preserve the series of level crossings but weaken the energy gap, and then (iii) impose Z_2-breaking perturbations.

V. *XXZ* MODEL

Our last model is the finite-size XXZ chains,

$$H_{XXZ} = \sum_{i=1}^{N-1} \Delta\left(\sigma_i^x\sigma_{i+1}^x + \sigma_i^y\sigma_{i+1}^y\right) + \sigma_i^z\sigma_{i+1}^z, \tag{28}$$

with N the length of the chains and Δ the anisotropic parameter. For $\Delta = 1$, the model reduces into the Heisenberg model and has an SU(2) symmetry. $\Delta_c = 1$ is also the critical point in the thermodynamic limit. For any $\Delta \neq 1$, the SU(2) symmetry is reduced into $U(1) \otimes Z_2$ symmetries. That is, the Hamiltonian remains unchanged when (i) the model is rotated around the z axis by any angle or (ii) the model is rotated around the x axis (or y axis) by π.

For the original XXZ chains without any perturbation, the nonlocality quantity $\mathcal{K}_{XXZ}(\Delta)$ is shown in Fig. 8.$\mathcal{K}_{XXZ}(\Delta)$ always presents a minimum at the critical point $\Delta_c = 1$. For $\Delta < 1$ and $\Delta > 1$, $\mathcal{K}_{XXZ}(\Delta)$ decreases and increases monotonously, respectively. Especially, when $N \to \infty$, one has $\mathcal{K}_{XXZ}(\Delta = 0) \to \frac{1}{2}$. It is quite clear that this situation with $\Delta = 0$ is physically equivalent to the transverse-field Ising chains with $\lambda \to \infty$.

We then consider a perturbed XXZ model given by

$$\tilde{H}_{XXZ} = H_{XXZ} + H'_z, \tag{29}$$

where H'_z denotes a staggered perturbation [67] which breaks the Z_2 symmetry and respects the U(1) symmetry,

$$H'_z = \delta \sum_{i=1}^{N} (-1)^i \sigma_i^z, \tag{30}$$

with $\delta = 10^{-4}$. The corresponding $\tilde{\mathcal{K}}_{XXZ}(\Delta)$ is shown in Fig. 8. It deserves mention that although the U(1) symmetry is involved, no oscillation is observed. The underlying reason is that the ground states of the XXZ chains are confined to the $\sum_i \sigma_i^z = 0$ subspace, which prevents them from undergoing a series of level crossings as in the XY chains.

We shall discuss the whole $\tilde{\mathcal{K}}_{XXZ}(\Delta)$ curve in Fig. 8 in three parts: $\Delta \approx 1$, $\Delta \ll 1$, and $\Delta \gg 1$. First, for $\Delta \approx 1$, the ground state is protected by the SU(2) symmetry (i.e., ΔE is large and thus $\frac{\delta}{\Delta E}$ is weak) and suffers little influence from the slight perturbation. Thus we find $\tilde{\mathcal{K}}_{XXZ}(\lambda) \approx \mathcal{K}_{XXZ}(\lambda)$. Second, in the large-$\Delta$ regions, according to Eq. (28), the in-plane U(1)-invariant term $\sum \sigma_i^x\sigma_{i+1}^x + \sigma_i^y\sigma_{i+1}^y$ (that is, the XX term) plays a major role. We have mentioned in the previous section that the energy gap ΔE of the XX model is also large. Consequently, for $\Delta \gg 1$ one also sees $\tilde{\mathcal{K}}_{XXZ}(\lambda) \approx \mathcal{K}_{XXZ}(\lambda)$. Third, in the small-$\Delta$ regions, according to Eq. (28), the Z_2-invariant term $\sum \sigma_i^z\sigma_{i+1}^z$ plays a major role, where the ground states tend to be doubly degenerate. In this situation, it is expected that the ground states can easily be destroyed by the Z_2-breaking perturbation H'_z. Thus, one can see that the nonlocality for $\Delta \ll 1$ is dramatically destroyed by the perturbation. As a result, $\tilde{\mathcal{K}}_{XXZ}(\Delta)$ presents an additional peak at some $\Delta = \Delta_{\text{peak}}$ with $0 < \Delta_{\text{peak}} < 1$.

It may be interesting to investigate whether this peak point would approach the critical point $\Delta_c = 1$ in the large-N limit. Thus, we have carried out scaling analysis upon the location of the peak; see Fig. 9. Using the data dots with $N = 30, 40,$ and 50, linear fitting gives $\Delta_{\text{peak}} = -7.469\frac{1}{N} + 0.6484$ (the red solid line). Using the data dots with $N = 10, 20, 30, 40,$ and 50, linear fitting gives $\Delta_{\text{peak}} = -6.139\frac{1}{N} + 0.6165$ (the blue dashed line). These fitting results suggest that in the large-N limit, the peak would not locate at the critical point $\Delta_c = 1$. Therefore, we expect that this perturbation-induced peak would survive in the large-N limit.

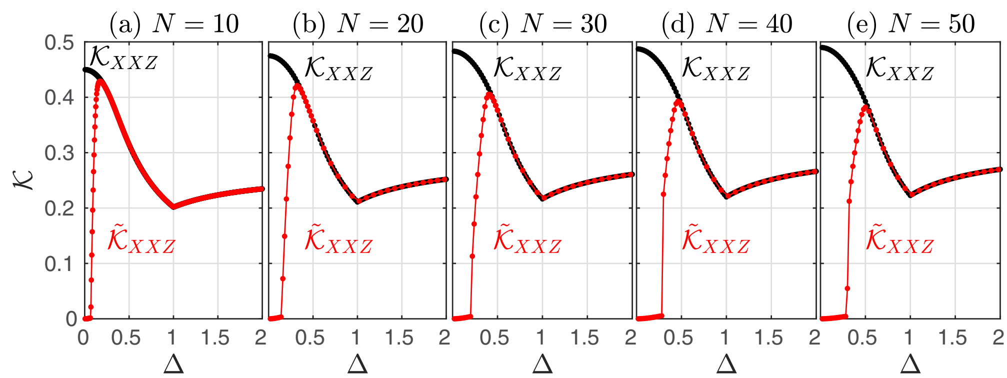

FIG. 8. Multipartite nonlocality in finite-size XXZ chains, $H = \Delta \sum(\sigma_i^x \sigma_{i+1}^x + \sigma_i^y \sigma_{i+1}^y) + \sum \sigma_i^z \sigma_{i+1}^z$, with N the length of the chains and Δ the anisotropic parameter. $\Delta_c = 1$ is the critical point in the thermodynamic limit. $\mathcal{K}_{XXZ}(\Delta)$ presents a valley at $\Delta_c = 1$. When a staggered perturbation $H_z' = \delta \sum(-1)^i \sigma_i^z$ with $\delta = 10^{-4}$ is imposed, nonlocality is destroyed dramatically in the weak-Δ regions, and then $\tilde{\mathcal{K}}_{XXZ}(\Delta)$ presents a perturbation-induced peak in the region $0 < \Delta < 1$.

VI. SUMMARY AND DISCUSSION

In this paper we have theoretically investigated the influence of symmetry-breaking perturbations upon ground-state nonlocality in several typical finite-size 1D quantum models, including the transverse-field Ising chains, the $XY(XX)$ chains, and the XXZ chains. We mention that multipartite nonlocality in these models have been studied extensively in previous works [51,53,59,60,74]. Nevertheless, part of the underlying mechanisms behind these earlier observations remained unclear. In this paper, by considering symmetry-breaking perturbations, some previously observed behaviors have been reproduced, and the corresponding mechanisms have been clarified. We shall discuss each of these behaviors in detail.

The first result deserving discussion is about the conflicting results in the transverse-field Ising chains. Reference [53] reported that in the finite-size situation, genuine n-partite nonlocality was observed and the nonlocality curve was a monotonous curve, while Refs. [51,59] reported that in the infinite-size situation, genuine nonlocality was not observed and the nonlocality curve presented a peak. The underlying mechanism for these two sets of conflicting results remained unclear.

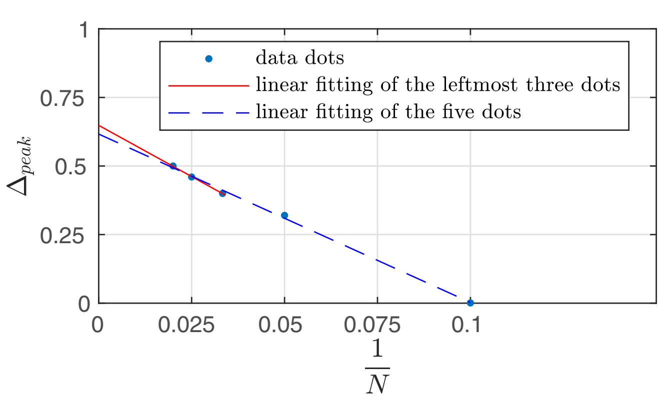

FIG. 9. Scaling analysis of the location of the perturbation-induced peak in the $\tilde{\mathcal{K}}_{XXZ}(\Delta)$ curve in Fig. 8. Linear fitting suggests that in the large-N limit, the peak would not locate at the critical point $\Delta_c = 1$.

In this paper, similar conflicting behaviors have been reproduced by considering Z_2-symmetry-breaking perturbations in finite-size chains; see Fig. 2. This shows ambiguously that in *finite*-size quantum chains, Z_2-symmetry breaking can reshape the property of multipartite nonlocality dramatically.

One may argue that what people are more interesting in would be *infinite*-size quantum chains *without any artificial perturbation,* as have been studied in Refs. [51,59]. We mention that the results reported in this paper can be easily extrapolated to infinite-size chains with $\delta \to 0$. Let us resort to the relative perturbation strength with respect to the energy gap, $\frac{\delta}{\Delta E}$, which determines the influence of the symmetry-breaking perturbation upon the ground-state nonlocality. In the Ising chains, for $\lambda < \lambda_c$, ΔE keeps finite in the large-N limit. Therefore, when the symmetry-breaking perturbation tends to vanish ($\delta \to 0$), one would have $\frac{\delta}{\Delta E} \to 0$, and thus the nonlocality should suffer no influence from the perturbation. For $\lambda > \lambda_c$, it is well known that the ground states are doubly degenerate ($\Delta E = 0$). Therefore, even if $\delta \to 0$, $\frac{\delta}{\Delta E}$ would not vanish, and thus the nonlocality may suffer dramatic influence and be destroyed. In this way, it is quite reasonable that the single-peak curve observed in the finite-size chains under Z_2-symmetry-breaking perturbations (Fig. 2) can survive in infinite-size chains with $\delta \to 0$. Therefore, we believe the key mechanism for the single-peak nonlocality curve (and consequently the vanish of genuine n-partite nonlocality in the large-λ limit) in infinite-size Ising chains [51,59] is the Z_2 symmetry and its breaking.

The second result deserving mention is about the XXZ chains. In Refs. [51,60] multipartite nonlocality in infinite-size XXZ chains was studied, and it was found that in the gapped antiferromagnetic phase (corresponding to $\Delta < \Delta_c = 1$ for the XXZ model consider in this paper), the nonlocality curve presented a peak. This peak did not attract much attention, and its underlying mechanism remained unclear. In this paper, this peak has also been successfully reproduced by considering Z_2-symmetry-breaking perturbations in finite-size XXZ chains (Fig. 8). Therefore, just as in the Ising model, we believe the corresponding peak in the nonlocality curve in the infinite-size XXZ chains [51,60] is also related to the Z_2 symmetry and its breaking.

The third behavior to be discussed is about the oscillation in the nonlocality curves. In Refs. [54] and [74], similar oscillation behaviors were observed in a spin ladder and an XX chain, respectively. Due to a lack of understanding of the underlying mechanism, Ref. [74] merely summarized the commonality between the spin ladder and the XX chain, i.e., U(1) symmetry was present and an external magnetic field was imposed. Nevertheless, the underlying function of the symmetry and the magnetic field in generating the oscillation was unclear.

In this paper we reveal that the presence of the U(1) symmetry and the magnetic field is to make sure that the ground states can undergo a series of level crossings. Furthermore, we show ambiguously that even if the U(1) symmetry is slightly broken (and is reduced into a Z_2 symmetry), the oscillation behavior can still be observed by a further breaking of the Z_2 symmetry (Figs. 3, 6, and 7). Thus, the research about the U(1) and Z_2 symmetries and their breaking not only reveals the underlying mechanisms of the oscillation behavior but also expands the scope in which the oscillation can occur.

Therefore, compared to previous works, the main contribution of this paper is that we have uncovered the important roles of symmetries and their breaking in ground-state multipartite nonlocality, which are ignored in previous papers.

We next provide a summary of this paper from the perspectives of general microscopic mechanisms and macroscopic symmetries. With the following summary, one shall be able to make some reliable predictions about multipartite nonlocality for some concerned quantum model by analyzing its microscopic energy levels or macroscopic symmetries.

Microscopically, the influence of the perturbation upon the ground-state nonlocality can be evaluated by the relative perturbation strength $\frac{\delta}{\Delta E}$. When $\frac{\delta}{\Delta E} \to 0$ (for instance, in the XX chains, ΔE is rather large), the perturbation effect would be weak. When $\frac{\delta}{\Delta E} \to \infty$ (for instance, in the transverse-field Ising chains with large λ, $\Delta E \to 0$), the perturbation effect would be significant. Furthermore, for models which have a series of ground-state level crossings, in the vicinity of each level-crossing point, $\frac{\delta}{\Delta E}$ is so large that the perturbation can dramatically destroy the ground state. Consequently, oscillations would be observed.

Macroscopically, symmetries and their breaking can dramatically reshape the behavior of multipartite nonlocality in 1D quantum chains. First, the breaking of the discrete Z_2 symmetry plays a *central* role. Explicitly, suppose the following three conditions are satisfied: (i) the original chain has a Z_2 symmetry, (ii) a Z_2-breaking perturbation is present, and (iii) the relative perturbation strength $\frac{\delta}{\Delta E}$ is large enough. Then the ground state and its nonlocality can be easily destroyed. This is just the situation in the transverse-field Ising chains with $\lambda > \lambda_c = 1$, the XY chains with $\lambda > \lambda_c = 1$, and the XXZ chains with $\Delta \ll \Delta_c = 1$. Second, in addition to the discrete Z_2 symmetry, the continuous U(1) symmetry also plays an *interesting* role. For instance, in the XX chains, because of the U(1) symmetry, the ground states undergo a series of level crossings. When anisotropy is considered, the U(1) symmetry would decrease into the Z_2 symmetry, and meanwhile the series of level crossings can be preserved and the energy gap is weakened. Then, when a Z_2-symmetry-breaking perturbation is present, at each of these level-crossing point, the three conditions can be satisfied, and thus the ground state and its nonlocality would be destroyed. Consequently, perturbation-induced oscillations emerge in the nonlocality curve. We expect that similar behaviors would be observed in quantum models which have similar symmetries.

The line of this work is far from finished. (1) First, we have studied just the influence of symmetry breaking upon *global* nonlocality of the ground states $|\psi_g\rangle$ in this paper. In a real Bell experiment upon solid materials, limited by the experimental conditions, one may just be able to carry out a Bell measure upon a certain subsystem, rather than the entire material. Thereby, a study on the influence of symmetry breaking upon *subchain* nonlocality (defined upon the reduced density matrix $\hat{\rho}_n$ of the concerned subsystem) in 1D quantum chains may be valuable. (2) In the entire physical picture, another fragment which is still missing is about the relation between the global nonlocality and subchain nonlocality. For instance, in the transverse-field Ising model, subchain nonlocality exhibits a single-peak curve [51], and global nonlocality can reproduce this behavior only if a Z_2-symmetry-breaking perturbation is imposed (Fig. 2). A similar phenomenon also exists in the XX model, where subchain nonlocality exhibits a oscillation behavior [74], and global nonlocality can reproduce this behavior only if symmetry-breaking perturbations are imposed (Fig. 3). This symmetry-breaking-induced similarity between global nonlocality and subchain nonlocality is a bit peculiar, and both a mathematical structure and a physical mechanism to explain this behavior are still missing and deserve some further revisiting. (3) Third, for typical 1D quantum chains with short-range interactions, only discrete symmetries (such as the Z_2 symmetry) may be spontaneously broken in infinite-size chains. That is why in the finite-size situation the ground-state nonlocality can be destroyed dramatically by Z_2-symmetry-breaking perturbations. When long-range interactions are taken into account, continuous symmetries [such as the U(1) symmetry] may also be spontaneously broken [82]. Therefore, it is expected that the breaking of the U(1) symmetry may play an even more interesting role in multipartite nonlocality in long-range interacting quantum chains, and may also deserve investigation. We will consider these issues in our future studies.

ACKNOWLEDGMENT

The research was supported by the National Natural Science Foundation of China (Grant No. 11675124).

[1] G. F. A. Osterloh, L. Amico and R. Fazio, Nature (London) **416**, 608 (2002).

[2] J. Eisert, M. Cramer, and M. B. Plenio, Rev. Mod. Phys. **82**, 277 (2010).

[3] G. Vidal, J. I. Latorre, E. Rico, and A. Kitaev, Phys. Rev. Lett. **90**, 227902 (2003).
[4] S.-J. Gu, S.-S. Deng, Y.-Q. Li, and H.-Q. Lin, Phys. Rev. Lett. **93**, 086402 (2004).
[5] S.-S. Deng, S.-J. Gu, and H.-Q. Lin, Phys. Rev. B **74**, 045103 (2006).
[6] R. Orús, Ann. Phys. **349**, 117 (2014).
[7] B. Bauer, L. D. Carr, H. G. Evertz, A. Feiguin, J. Freire, S. Fuchs, L. Gamper, J. Gukelberger, E. Gull, S. Guertler *et al.*, J. Stat. Mech.: Theory Exp. (2011) P05001.
[8] M. Fishman, S. R. White, and E. M. Stoudenmire, The ITensor software library for tensor network calculations, SciPost Phys. Codebases **4** (2022).
[9] P. van Loock and S. L. Braunstein, Phys. Rev. Lett. **84**, 3482 (2000).
[10] M. Bourennane, M. Eibl, C. Kurtsiefer, S. Gaertner, H. Weinfurter, O. Gühne, P. Hyllus, D. Bruß, M. Lewenstein, and A. Sanpera, Phys. Rev. Lett. **92**, 087902 (2004).
[11] G. L. Giorgi, B. Bellomo, F. Galve, and R. Zambrini, Phys. Rev. Lett. **107**, 190501 (2011).
[12] G. Tóth, Phys. Rev. A **85**, 022322 (2012).
[13] F. Levi and F. Mintert, Phys. Rev. Lett. **110**, 150402 (2013).
[14] Y.-K. Bai, N. Zhang, M.-Y. Ye, and Z. D. Wang, Phys. Rev. A **88**, 012123 (2013).
[15] T. Fritz, A. Sainz, R. Augusiak, J. B. Brask, R. Chaves, A. Leverrier, and A. Acin, Nat. Commun. **4**, 2263 (2013).
[16] M. Chen, N. C. Menicucci, and O. Pfister, Phys. Rev. Lett. **112**, 120505 (2014).
[17] S. Armstrong, M. Wang, R. Y. Teh, Q. Gong, Q. He, J. Janousek, H.-A. Bachor, and M. D. R. . P. K. Lam, Nat. Phys. **11**, 167 (2015).
[18] P. Hauke, M. Heyl, L. Tagliacozzo, and P. Zoller, Nat. Phys. **12**, 778 (2016).
[19] G. D. Chiara and A. Sanpera, Rep. Prog. Phys. **81**, 074002 (2018).
[20] N. D. Mermin, Phys. Rev. Lett. **65**, 1838 (1990).
[21] A. V. Belinskii and D. N. Klyshko, Phys. Usp. **36**, 653 (1993).
[22] V. Scarani and N. Gisin, J. Phys. A: Math. Gen. **34**, 6043 (2001).
[23] H. Weinfurter and M. Żukowski, Phys. Rev. A **64**, 010102(R) (2001).
[24] R. F. Werner and M. M. Wolf, Phys. Rev. A **64**, 032112 (2001).
[25] M. Żukowski and Č. Brukner, Phys. Rev. Lett. **88**, 210401 (2002).
[26] J.-D. Bancal, C. Branciard, N. Gisin, and S. Pironio, Phys. Rev. Lett. **103**, 090503 (2009).
[27] J. Batle and M. Casas, Phys. Rev. A **82**, 062101 (2010).
[28] E. G. Cavalcanti, Q. Y. He, M. D. Reid, and H. M. Wiseman, Phys. Rev. A **84**, 032115 (2011).
[29] J.-D. Bancal, N. Brunner, N. Gisin, and Y.-C. Liang, Phys. Rev. Lett. **106**, 020405 (2011).
[30] N. Brunner, J. Sharam, and T. Vértesi, Phys. Rev. Lett. **108**, 110501 (2012).
[31] N. Brunner, D. Cavalcanti, S. Pironio, V. Scarani, and S. Wehner, Rev. Mod. Phys. **86**, 419 (2014).
[32] J.-D. Bancal, J. Barrett, N. Gisin, and S. Pironio, Phys. Rev. A **88**, 014102 (2013).
[33] J. Tura, R. Augusiak, A. B. Sainz, T. Vértesi, M. Lewenstein, and A. Acin, Science **344**, 1256 (2014).
[34] Q. Chen, S. Yu, C. Zhang, C. H. Lai, and C. H. Oh, Phys. Rev. Lett. **112**, 140404 (2014).
[35] J. Bowles, J. Francfort, M. Fillettaz, F. Hirsch, and N. Brunner, Phys. Rev. Lett. **116**, 130401 (2016).
[36] R. Schmied, J.-D. Bancal, B. Allard, M. Fadel, V. Scarani, P. Treutlein, and N. Sangouard, Science **352**, 441 (2016).
[37] A. de Rosier, J. Gruca, F. Parisio, T. Vértesi, and W. Laskowski, Phys. Rev. A **96**, 012101 (2017).
[38] J. Tura, G. De las Cuevas, R. Augusiak, M. Lewenstein, A. Acín, and J. I. Cirac, Phys. Rev. X **7**, 021005 (2017).
[39] F. Baccari, J. Tura, M. Fadel, A. Aloy, J.-D. Bancal, N. Sangouard, M. Lewenstein, A. Acín, and R. Augusiak, Phys. Rev. A **100**, 022121 (2019).
[40] A. Aloy, J. Tura, F. Baccari, A. Acín, M. Lewenstein, and R. Augusiak, Phys. Rev. Lett. **123**, 100507 (2019).
[41] A. Piga, A. Aloy, M. Lewenstein, and I. Frérot, Phys. Rev. Lett. **123**, 170604 (2019).
[42] P. Contreras-Tejada, C. Palazuelos, and J. I. de Vicente, Phys. Rev. Lett. **126**, 040501 (2021).
[43] V. Gebhart, L. Pezzè, and A. Smerzi, Phys. Rev. Lett. **127**, 140401 (2021).
[44] M. Pandit, A. Barasiński, I. Márton, T. Vértesi, and W. Laskowski, New J. Phys. **24**, 123017 (2022).
[45] C. Zhang, C.-J. Zhang, Y.-F. Huang, Z.-B. Hou, B.-H. Liu, C.-F. Li, and G.-C. Guo, Sci. Rep. **6**, 39327 (2016).
[46] M. Giustina, A. Mech, S. Ramelow, B. Wittmann, J. B. J. Kofler, A. Lita, B. Calkins, T. Gerrits, S. W. Nam, R. Ursin, and A. Zeilinger, Nature (London) **497**, 227 (2013).
[47] J.-W. Pan, D. Bouwmeester, M. Daniell, H. Weinfurter, and A. Zeilinger, Nature (London) **403**, 515 (2000).
[48] M. A. Rowe, D. Kielpinski, V. Meyer, C. A. Sackett, W. M. Itano, C. Monroe, and D. J. Wineland, Nature (London) **409**, 791 (2001).
[49] B. P. Lanyon, M. Zwerger, P. Jurcevic, C. Hempel, W. Dür, H. J. Briegel, R. Blatt, and C. F. Roos, Phys. Rev. Lett. **112**, 100403 (2014).
[50] S. Campbell and M. Paternostro, Phys. Rev. A **82**, 042324 (2010).
[51] Z.-Y. Sun, B. Guo, and H.-L. Huang, Phys. Rev. A **92**, 022120 (2015).
[52] Y. Dai, C. Zhang, W. You, Y. Dong, and C. H. Oh, Phys. Rev. A **96**, 012336 (2017).
[53] Z.-Y. Sun, M. Wang, Y.-Y. Wu, and B. Guo, Phys. Rev. A **99**, 042323 (2019).
[54] H.-G. Cheng, M. Li, Y.-Y. Wu, M. Wang, D. Zhang, J. Bao, B. Guo, and Z.-Y. Sun, Phys. Rev. A **101**, 052116 (2020).
[55] J. Bao, B. Guo, H.-G. Cheng, M. Zhou, J. Fu, Y.-C. Deng, and Z.-Y. Sun, Phys. Rev. A **101**, 012110 (2020).
[56] Z.-Y. Sun, H.-X. Wen, M. Li, and B. Guo, Phys. Rev. A **105**, 012213 (2022).
[57] L. Justino and T. R. de Oliveira, Phys. Rev. A **85**, 052128 (2012).
[58] D.-L. Deng, C. Wu, J.-L. Chen, S.-J. Gu, S. Yu, and C. H. Oh, Phys. Rev. A **86**, 032305 (2012).
[59] Z.-Y. Sun, Y.-Y. Wu, J. Xu, H.-L. Huang, B.-F. Zhan, B. Wang, and C.-B. Duan, Phys. Rev. A **89**, 022101 (2014).
[60] Z.-Y. Sun, S. Liu, H.-L. Huang, D. Zhang, Y.-Y. Wu, J. Xu, B.-F. Zhan, H.-G. Cheng, C.-B. Duan, and B. Wang, Phys. Rev. A **90**, 062129 (2014).
[61] Z.-Y. Sun, H.-X. Wen, M. Li, and Y. Li, Phys. Rev. A **104**, 052202 (2021).
[62] Z.-Y. Sun, X. Guo, and M. Wang, Eur. Phys. J. B **92**, 75 (2019).

[63] L. Šmejkal, R. González-Hernández, T. Jungwirth, and J. Sinova, Sci. Adv. **6**, eaaz8809 (2020).
[64] A. Galda and V. M. Vinokur, Phys. Rev. B **97**, 201411(R) (2018).
[65] K. Karľová, J. Strečka, and M. L. Lyra, Phys. Rev. B **97**, 104407 (2018).
[66] G. L. Giorgi, Phys. Rev. B **82**, 052404 (2010).
[67] O. F. Syljuåsen, Phys. Rev. A **68**, 060301(R) (2003).
[68] A. Osterloh, G. Palacios, and S. Montangero, Phys. Rev. Lett. **97**, 257201 (2006).
[69] T. R. de Oliveira, G. Rigolin, M. C. de Oliveira, and E. Miranda, Phys. Rev. A **77**, 032325 (2008).
[70] L. J. Pereira and T. R. de Oliveira, Front. Phys. **4** (2016).
[71] J.-H. Zhao, H.-L. Wang, B. Li, and H.-Q. Zhou, Phys. Rev. E **82**, 061127 (2010).
[72] A. Z. D. M. Greenberger, M.A. Horne, *Bell's Theorem, Quantum Theory, and Conceptions of the Universe* (Academic Press, Dordrecht, 1989).
[73] W. Dür, G. Vidal, and J. I. Cirac, Phys. Rev. A **62**, 062314 (2000).
[74] Z.-Y. Sun, M. Li, L.-H. Sheng, and B. Guo, Phys. Rev. A **103**, 052205 (2021).
[75] J. Batle and M. Casas, J. Phys. A: Math. Theor. **44**, 445304 (2011).
[76] T. R. de Oliveira, A. Saguia, and M. S. Sarandy, EPL (Europhys. Lett.) **100**, 60004 (2012).
[77] F. Altintas and R. Eryigit, Ann. Phys. **327**, 3084 (2012).
[78] D. Collins, N. Gisin, S. Popescu, D. Roberts, and V. Scarani, Phys. Rev. Lett. **88**, 170405 (2002).
[79] Q. Y. He, E. G. Cavalcanti, M. D. Reid, and P. D. Drummond, Phys. Rev. Lett. **103**, 180402 (2009).
[80] X. Wang, C. Zhang, Q. Chen, S. Yu, H. Yuan, and C. H. Oh, Phys. Rev. A **94**, 022110 (2016).
[81] G.-B. Xu, Q.-Y. Wen, S.-J. Qin, Y.-H. Yang, and F. Gao, Phys. Rev. A **93**, 032341 (2016).
[82] M. F. Maghrebi, Z.-X. Gong, and A. V. Gorshkov, Phys. Rev. Lett. **119**, 023001 (2017).